

Received August 28, 2021, accepted September 9, 2021, date of publication September 10, 2021, date of current version September 21, 2021.

Digital Object Identifier 10.1109/ACCESS.2021.3112069

# Hybrid Local-Global Optimum Search Using Particle Swarm Gravitation Search Algorithm (HLGOS-PSGSA) for Waveguide Selection

SIMARPREET KAUR<sup>1</sup>, MOHIT SRIVASTAVA<sup>2</sup>,  
NAVEEN KUMAR SHARMA<sup>1</sup>, (Senior Member, IEEE),  
KAMALJIT SINGH BHATIA<sup>3</sup>, (Senior Member, IEEE),  
FRIE AYALEW YIMAM<sup>4</sup>, HARSIMRAT KAUR<sup>5</sup>,  
AND MOHIT BAJAJ<sup>6</sup>, (Member, IEEE)

<sup>1</sup>Department of Electrical Engineering, I. K. Gujral Punjab Technical University, Jalandhar 144603, India

<sup>2</sup>ECE Department, Chandigarh Engineering College, Landran, Punjab 140307, India

<sup>3</sup>Department of ECE, G. B. Pant Institute of Engineering & Technology, Pauri, Garhwal 246194, India

<sup>4</sup>School of Electrical and Computer Engineering, Woldia University, Woldia 67815, Ethiopia

<sup>5</sup>Department of ECE, CT Institute of Engineering and Technology, Jalandhar, Punjab 144623, India

<sup>6</sup>Department of Electrical and Electronics Engineering, National Institute of Technology Delhi, New Delhi 110040, India

Corresponding author: Frie Ayalew Yimam (frie.ayalew@aastu.edu.et)

**ABSTRACT** Multiple beam combination in optical interferometry with concurrent measurement of intricate visibilities, around each possible baseline, is a trending research area. In this work, a hybrid method is proposed for three different waveguide arrays and several waveguides are excited simultaneously in each array. Each waveguide array acts as a beam combiner, the output of which determines the field intensity of each waveguide mode. The output intensity depends on the waveguide selected for excitation. Thus, waveguide selection is the major factor that can affect the output intensity. The main goal of this research is to provide an effective solution for the selection of waveguides, to provide high visibility and intensity at the output of the multi-beam combiner. In addition to this, the use of metaheuristic optimization algorithms to solve the problem of waveguide selection is proposed. To accomplish this, firstly, an analytical study has been conducted to analyze the performance of optimization algorithms, including PSO, FA and GSA, and then the results of these algorithms have been compared with the conventional approaches. And finally, a model of Hybrid Local-Global Optimum Search Algorithm using Particle Swarm Gravitation Search Algorithm (HLGOS-PSGSA) has been developed for waveguide selection. The performance of the proposed hybrid model is examined in MATLAB simulation software. The simulated outcomes are determined for PSO, FA, and GSA-based models, as well as, for the proposed hybrid model, in terms of normalized intensity, visibility, and min-max  $1/\text{SNR}$  values. The results obtained from simulation show that the PSO and GSA-based models are giving better results, followed by FA and conventional approaches. This worked as a motivation behind using PSO and GSA together in the proposed system, resulting in higher intensity and visibility values. Thus, the proposed hybrid model is concluded to be more efficient and convenient, for selecting optimum waveguides from the array, to attain an optimum output.

**INDEX TERMS** Interferometers, MZI, waveguide array, waveguide selection, PSO, intensity, visibility, SNR.

The associate editor coordinating the review of this manuscript and approving it for publication was Seyedali Mirjalili.

## I. INTRODUCTION

Interferometers are devices that produce interference among two or more waves. Thus, they are used in the study of interference patterns generated by different light sources. They are

of various kinds, with different characteristics, and can use multiple beams [1].

The angular resolution of the optical system having size  $d$ , performed at wavelength  $\lambda$ , is restricted by diffraction to  $\approx \lambda/d$ . Therefore, high resolution means huge optical systems. Every time the enviable resolution goes beyond the confines of monolithic telescopes which are well-sized, the entry aperture should be divided into various tiny collectors, separate beams of which must be joined comprehensively. These kinds of systems are referred to as astronomical interferometers [2]. In Fig. 1, the simplest notion of these systems is represented. As shown in the figure, the most significant components of the astronomical interferometer are the two telescopes or siderostats, delay lines that can be moved for equalizing the length of the optical path in two interferometer arms, a beam combiner, and the detectors [3].

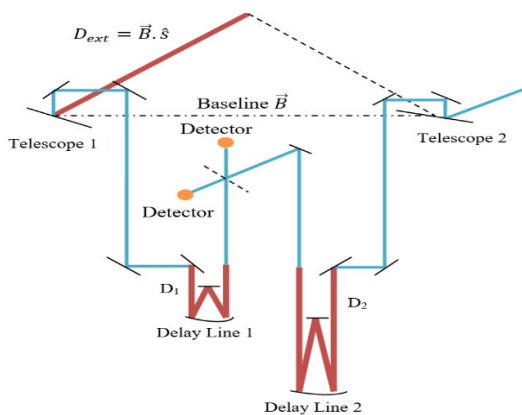


**FIGURE 1.** Schematic drawing of the light path through a two-element interferometer [3].

For astronomical objects' high-resolution imaging with the astronomical interferometers, dense sampling of their light coherence function is required. It is attained by evaluating the intricate visibilities of the interference fringes across a huge number of baselines. In optical interferometry, the recent trend is to perform multiple-beam combination with concurrent evaluation of intricate visibilities across every potential baseline subtended by the array of various telescopes [4]. This approach is mainly appropriate for fast-events observation, like photospheres of stars, nova/supernova explosions, or transits of exo-planets.

In this context, the technological solution i.e. integrated optics is ascertained for performing multiple-beam combinations in astronomical interferometers. Due to integrated optical interferometers' high stability in opposition to thermal changes and vibrations, they have great performance concerning phase measurement and visibility [5].

## II. PURPOSE OF THE INVESTIGATION

Multi-beam combination is the recent trend in interferometry that evaluates the visibility of the waveguides subtended by waveguide arrays. For this, the waveguide arrays with a different number of waveguides are taken, and from these

arrays, several waveguides are excited simultaneously. For the waveguide array to operate as an interferometry beam-combiner, the waveguides must be coupled beyond the nearest neighbor in the array [6]. Long-range coupling can be attained by placing the waveguides in a rectangular array. This will act as a beam combiner, which evaluates the intensity of each waveguide mode. The output intensity of the waveguide must be high to attain high output intensity [5]. And this output intensity depends upon the waveguides that have been selected and excited in the array. Thus, waveguides must be selected optimally, so that, the high-intensity output can be attained.

However, with the increase in the number of waveguides, the determination of waveguides for selection becomes complex [4]. Optimal selection of waveguides is the major problem that if solved, can result in the attainment of high-intensity levels at the output.

Thus, in this paper, the problem of waveguide selection, to attain high intensity at the output of the beam combiner, is the main emphasis.

For this, we have decided to implement the optimization algorithms for waveguide selection. Generally, the optimization algorithms help to determine the most optimal solution from the number of solutions provided. Inspired by this, we have considered the optimization algorithms for the proposed work with the intention that it will help to determine the most optimal waveguides from the number of presented waveguides. After that, a hybrid optimization algorithm on basis of the top two best-performing algorithms is also given in this study, which is simulated and analyzed in terms of intensity, visibility, and min-max 1/SNR. A comparison is also performed with the traditional approach optimization algorithms-based models, to show the effectiveness and improvement of the proposed scheme.

However, the selection of an optimization algorithm for this purpose is also the main concern. Several optimization algorithms such as GA (Genetic Algorithm) [7], [8], ACO (Ant Colony Optimization) [9], [10], ABC (Artificial Bee Colony) [11], PSO (Particle Swarm Optimization) [12] have been analyzed. GA uses particular generic operators like crossover, reproduction, and mutation to form a new population. It requires a limited set of parameters, but the major drawback is its slow convergence to the optimal solution, because of the random crossover and mutation processes [13], [14]. ACO was proposed by Macro Dorigo in 1992. It is a metaheuristic approach based on ants foraging behavior [15]. ACO is beneficial over other evolutionary approaches, as it offers positive feedback, which results in fast solution finding, and also avoids untimely convergence because of its dispersed computation. But, its main disadvantage is its slower convergence compared with the other evolutionary algorithms and the time for convergence is also uncertain. Its performance is poor in large search space problems [16]. ABC algorithm was proposed by Dervis Karaboga in 2005, and its performance was first analyzed in 2007 [17], from which it was established that ABC is

relatively better than several other evolutionary approaches [18]. It is motivated by the intelligent behavior of the honey bees in finding the food sources, i.e. nectar, and then sharing this information with other bees in the nest [19]. Its main advantages are that the implementation of this algorithm is as simple as that of PSO, it is highly flexible and robust. But, for better performance, it requires new fitness tests for new parameters and is also slow [20]. Recently, few algorithms other than nature-inspired ones, such as Stochastic Paint Optimizer (SPO) [21] and Flow Direction Algorithm (FDA), [22] which are inspired by art and physics-based algorithms, have been proposed. But such algorithms are not attaining much interest from researchers in comparison to nature-inspired algorithms. Other than these, GSA “Gravitational Search Algorithm” is a heuristic optimization method that takes each agent as an object that communicates among itself under gravitational force [23].

Since its development, Gravitational Search Algorithm has been suggested and utilized in a variety of sectors by integrating it with other optimization techniques. Merging two optimization techniques in a specific manner is one of the most significant changes. Following are some of the papers that serve as examples of hybrid algorithms: In [24], for the Automatic Generation Control issue, a hybrid Many Optimizing Liaisons Gravitational Search Algorithm (hMOL-GSA) based fuzzy PID controller is presented. The fuzzy PID parameters are tuned using the presented technique. The results were compared to those of the recently suggested Firefly Algorithm optimized PID and Teaching Learning Based Optimization (TLBO). The presented hMOL-GSA approach has been shown to improve system performance. The study in [25] provided a new image segmentation technique called GA-GSA (Genetic Algorithm-based Gravitational Search Algorithm). The outcomes achieved surpassed findings achieved using GSA (Genetic Search Algorithm) and PSO (Particle Swarm Optimization). A study by [26], utilized chaotic neural oscillators to update GSA-CNO, a gravitational constant. Experiments revealed that chaotic neural oscillators successfully adjusted the gravitational constant, allowing GSA-CNO to act well and maintain its reliability against four gravitational search algorithms variants on functions.

There are numerous examples of how to create a hybrid algorithm by mixing characteristics from two separate optimization techniques. The Grasshopper Optimization Algorithm (GOA) and the Bees Algorithm (BA) were used in this research to solve the deployment issue in WSNs [27]. The approach in [28] offers a unique hybrid technique for handling global optimization issues termed Whale Optimization with Seagull Algorithm (WSOA). Twenty-five benchmark test functions were used to examine the efficacy of addressing global optimization issues, and WSOA was compared to seven well-known metaheuristic methods. [29] proposed a new hybrid optimization technique relying on CSA “Clonal Selection Algorithm”, which combined the benefits of two existing optimization approaches,

PSO “Particle Swarm Optimization” and GBMO “Gases Brownian Motion Optimization”, to improve the quality of the initial population. The author of [30] presented a hybrid PSO-CS “Particle Swarm Optimization-Cuckoo Search” technique for addressing nonlinear optimization issues. A hybrid strategy was developed and subsequently utilized for clustering algorithm, combining adaptive elitist Differential Evolution (aeDE), a population-based technique, with SQSD “Spherical Quadratic Steepest Descent”, a powerful gradient-based technique in [31].

In [32], a new hybrid population-based algorithm (PSOGSA) has been introduced with the blend of the strengths of both PSO and GSA. The main motive behind combining these two algorithms is to synthesize the power of both the algorithms, by integrating the properties of PSO to exploit, and that of GSA to explore. In this research, some of the benchmark test functions have been used to compare the performance of hybrid PSOGSA with both PSO and GSA algorithms, in attaining the best solution. It has been proved that the hybrid algorithm is much better than the individual PSO and GSA algorithms in fast convergence, as well as, in function minimization. In yet another hybrid nature-inspired approach (MGBPSO-GSA) in [33], developed with a combination of Mean Gbest Particle Swarm Optimization (MGBPSO) and Gravitational Search Algorithm (GSA), it has been proved that the new hybrid approach outperforms considerably in various metaheuristics, in terms of solution quality, convergence speed, stability, and capability of a local and global optimum. The authors of [34] presented a new hybrid PSO-GSA technique for environmental/ economic dispatch problem, by combining PSO and GSA techniques, and have proved the effectiveness of the proposed algorithm over previous optimization methods. In another study in [35], a new hybrid PSOGSA algorithm for generating test data automatically has been proposed by combining the PSO and GSA algorithms. This hybrid PSOGSA algorithm has overcome the problem of PSO getting trapped in local minima, and GSA, having slow convergence, and thus, resulting in an efficient algorithm, proving that the hybrid PSOGSA is giving stable performance throughout the generations. It is presented that PSOGSA converges faster by covering all possible paths as compared to PSO and GSA. There are many such studies available, that reveal that hybridization of nature-inspired algorithms is an effective approach to merge advantages and strengths of individual algorithms for handling their insufficiencies.

From the literature survey, it can be seen that till now, most of the researchers are focusing on using popular optimization algorithms for initial analyzing, and solving the selected problems of different research areas. Few of them have tried to hybridize the top-performing algorithms out of chosen ones. In this paper, firstly, we are focusing on introducing the concept of optimization algorithms in waveguide selection. For this, the selected algorithms are PSO, FA, and GSA. Furthermore, after analyzing the performance of these optimization algorithms on performance

matrices, a hybrid model using PSO and GSA algorithms is proposed.

### III. DETAILS OF PSO, GSA, AND FIREFLY OPTIMIZATION ALGORITHMS

A brief about the existing PSO, GSA, and FA has been described in this section.

#### A. PARTICLE SWARM OPTIMIZATION ALGORITHM

Russell Eberhart and James Kennedy first proposed Particle Swarm Optimization (PSO) in 1995. PSO has recently acquired popularity due to its effectiveness in tackling complex and difficult optimization issues. PSO is utilized in a variety of applications like growing ANN (Artificial Neural Networks), cooperative communication network power allocation, character recognition, ML (Machine Learning), etc. Moreover, while tackling nonlinear, multi-modal and, non-differentiable issues, PSO has indeed been demonstrated to be both resilient and quick [36]. PSO calculates the best function value and placement for each particle location by evaluating the objective function. It determines fresh velocities based on existing velocity, the particle's novel location individually, and the optimal location of their neighbors. Then, iteratively modify the location of the particles (the new location is the same as the old one, but with a higher velocity, which has been tweaked for keeping particles inside the boundaries) [37]. Iterations continue until the algorithm hits a threshold for halting. The following is the technique for the PSO algorithm:

**Step1** Initially, the particles of size N, are generated randomly.

**Step 2** Set the velocity and location vectors of each particle,  $v_i$  and  $x_i$ , respectively, ( $i = \{1, 2, \dots, N\}$ ), and determine each particle's fitness in the population.

**Step 3** Select the most appropriate spot for each particle, based on its fitness ( $P_{bi}$ ,  $i \{1, 2, \dots, N\}$ ).

**Step 4** Set the ideal position for the entire swarm,  $G_b$  depending upon the fitness function.

**Step 5** Calculate each particle's new velocity  $v_{ij}^{t+1}$ , by utilizing equation

$$v_{ij}^{t+1} = v_{ij}^t + c_1 x (\text{random}(0, 1)) x (P_{bij}^t - x_{ij}^t) + c_2 x (\text{random}(0, 1)) (G_{bj}^t - x_{ij}^t),$$

$$j \in \{1, \dots, D\}, c_1 \text{ and } c_2 \quad (1)$$

between 0 and 1, that are positive random numbers.

**Step 6** As per  $x_{ij}^{t+1} = x_{ij}^t + v_{ij}^{t+1}$ ,  $j \in \{1, \dots, D\}$ , move each particle to the next location  $x_{ij}^{t+1}$ .

**Step7** If the iteration's number approaches the pre-determined maximum number of iterations,  $\text{maxCycle}$ , the iteration is ended. If not, proceed to step three.

#### B. GRAVITATIONAL SEARCH ALGORITHM

GSA is an effective heuristic optimization algorithm for non-linear optimization issues and provides excellent results.

Gravitational Search Algorithm is supported by the concept of mass interaction, which says that "a particle in the universe attracts every other particle with a strength which is inversely proportional to the square of the distance between them, and directly proportional to the multiplication of their masses" [38]. Individuals are regarded as objects in GSA. The mass of the object is utilized to determine the object's functionality. The heavier masses of the objects correspond to excellent solutions. Because of the gravitational pull, all objects with large masses attract objects with smaller masses, ensuring the method's exploration. Furthermore, object with heavier masses, i.e. good solutions, travel slower than objects with smaller masses [39]. Gravitational Search Algorithm, which is based on physics principles, outperformed other bio-inspired and nature-inspired methods like Harmony Search, Cat Swarm, PSO, and others in terms of functionality and features. Every agent is reproduced as a matter in Gravitational Search Algorithm, and the issue search region is the universe, in which they are subject to gravitational pull. The gravitational field is described as a curvature of space-time, according to Einstein's general theory of relativity. As a result, there are still plenty of possibilities to use gravity principles and develop innovative search tools in this research field. As a result, Gravitational Search Algorithm is regarded as both a population- and physics-based metaheuristic search method [40]. Following is the Gravitational Search Algorithm process:

**Step 1** In an 'n' agent system, declare the search space at random:

$$X = \{x_1, x_2, x_3, \dots, x_n\} \quad (2)$$

where (all agents attract the single heavy mass)

**Step 2** Compute  $m(t)$  (a fitness function)

**Step 3** Adjust  $G(t)$  (the gravitational constant)

**Step 4** Calculate  $F_{ij}$  (Gravitational force) by using equation (3)

$$F_{ij} = G(t) \frac{m_{pi}(t) m_{aj}(t)}{R_{ij}(t) + \epsilon} (x_j^d(t) + x_i^d(t)) \quad (3)$$

Here,  $R_{ij}(t)$  is the Euclidian distance,  $m_{aj}(t)$  is the active gravitational mass, and  $m_{pi}(t)$  is the passive gravitational mass.  $M$  is a constant with a small value in 'd' dimensional space.

**Step 5** Using equation (4), compute the acceleration,  $a_i^d(t)$

$$a_i^d(t) = \frac{F}{M} \quad (4)$$

As per the force law of motion, "The acceleration (a) of the agent is inversely proportional to the M "mass of the agent" and directly related to the F "force applied by the agent".

**Step 6** Adjust the agent locations:  $x_i^d(t+1)$  and the velocity:  $v_i^d(t+1)$  by

$$v_i^d(t+1) = \text{random}(0, 1) x v_i^d(t) + a_i^d(t) \quad (5)$$

$$x_i^d(t+1) = x_i^d(t) + v_i^d(t+1) \quad (6)$$



**Step 7** If the number of iterations exceeds the highest limit of iterations, the loop is stopped, and RETURN the strongest candidate response. Otherwise, return to step one.

### C. FIREFLY OPTIMIZATION ALGORITHM

Yang created the Firefly Algorithm (a revolutionary swarm intelligent optimization scheme) in 2008, after analyzing the movement mechanism and mutual attraction of firefly individuals (FA). Because, the Firefly Algorithm has the benefits of a basic concept, ease of deployment, less parameter impact on the method, and fewer parameters to specify [41]. As a result, the firefly algorithm is a heuristic method designed to mimic the biological properties of adult insect luminescence in the environment. This is also a group-based random optimization technique. Every firefly sends luciferin to interact with other fireflies to discover food and mating throughout their collecting operations. The brighter the luciferin, the more attractive the firefly becomes, and ultimately a large number of fireflies would congregate around the firefly with the luciferin [42]. Firefly algorithm has been used to solve a variety of optimization issues including production planning, stock forecasting, and structure design [43]. Firefly is dependent on attraction, which is utilized by fireflies to travel towards greater light intensity. The change of light intensity and the formulation of attraction are two crucial qualities that firefly provides to overcome optimization issues [44]. The Gravitational Search Algorithm method was outlined as follows:

**Step 1:** Produce initial firefly population  $x_i$ , where ( $i = 1, 2, 3, N$ ). Light intensity  $l_i$  at  $x_i$  is discovered by  $f(x_i)$ .

**Step 2:** State “ $\gamma$ ”, the light absorption coefficient, and IN “the number of iterations”.

**Step 3:** Estimate the fitness function for fireflies utilizing the objective function.

**Step 4:** Adjust the firefly’s light intensity.

**Step 5:** Sort the fireflies into various categories and choose the best.

**Step 6:** Move the fireflies for a good result.

**Step 7:** If the number of iterations exceeds the highest limit of iterations, the loop is terminated, and RETURN the optimum solution. Otherwise, continue with step 3 again.

## IV. PROPOSED MODEL: HYBRID LOCAL-GLOBAL OPTIMUM SEARCH USING PARTICLE SWARM GRAVITATION SEARCH ALGORITHM (HLGOS-PSGSA) FOR WAVEGUIDE SELECTION

As discussed in the above sections, the existing interferometry beam-combiners have waveguides that help in achieving a combined beam at the screen with different intensities. Therefore, the selection of the waveguides is an important factor that is to be considered. This section provides details of the proposed Hybrid Local-Global Optimum Search using Particle Swarm Gravitation Search Algorithm (HLGOS-PSGSA). PSO is proved to be better in finding global optima, and faces fewer issues in local solution [52]–[53], whereas, GSA falls into the local optimal solution more easily, which greatly

reduces the exploration capability of the algorithm [54], [55]. Therefore, for combining PSO and GSA features, the scenario given in equation (1) is updated in this study. We have updated the velocity updating phase of PSO, by including the GSA local search capability. The updated velocity factor of the proposed scheme is given as below:

$$Vu_{ij}^{t+1} = v_{ij}^t + c_1 \times \text{random}(0, 1) \times (ac_{ij}^t) + c_2 \times \text{random}(0, 1) \times (Gb_j^t - x_{ij}^t) \quad (7)$$

where,  $Vu_{ij}^{t+1}$  is the updated velocity factor, calculated in every iteration of PSO to update the population. Normally, the local best of PSO is updated by using a difference of best and current location, as given in equation (1), i.e.  $(Pb_{ij}^t - x_{ij}^t)$ . Here, we have used the acceleration factor of GSA to optimize the search.

After achieving the optimized velocity, the position of the particles is updated by

$$x_{ij}^{t+1} = x_{ij}^t + Vu_{ij}^{t+1} \quad (8)$$

### A. METHODOLOGY

The description of the process of selection of waveguides is explained below:

**Step 1:** Initialization of the proposed model’s initial factors, such as number of iterations to run, the initial population in terms of waveguide numbers, particle’s velocity, etc.

**Step 2:** Next step is to evaluate the initial population generated in the fitness function.

Here, the fitness function is calculated in terms of summation of intensity by following the below-written equations (9) and (10):

$$I = \sum_{j=1}^N \sum_{k=1}^N \alpha_{m,f(j)} \alpha_{m,f(k)}^* \langle A_j A_k^* \rangle \quad (9)$$

$$\text{fitness} = \sum_{j=1}^n I_j \quad (10)$$

where  $n$  is the number of waveguides to be selected.

The intensity is calculated by using equation (1). Firstly, the intensity of the individual waveguides is calculated, and then, for the overall improvement, the sum of intensities is taken as fitness in the proposed model.

**Step 3:** After evaluating the initial fitness, local best is calculated with high fitness, and a population with overall high fitness is saved in  $gbest$ .

**Step 4:** This  $gbest$  is the best-fitted population for the current iteration, which will be compared in the rest of the iterations until all iterations are done.

**Step 5:** Next phase is to update the initial population by using velocity update equation (7), in which the acceleration factor is determined by using equation (4).

**Step 6:** After updating the velocity factor, the population for the next iteration is updated by using equation (8).

**Step 7:** Once all iterations are completed, the final gbest is considered to be the final output as the selected waveguide number.

Now, to analyze this, a different number of waveguide scenarios are considered i.e.  $2 \times 2$ ,  $3 \times 3$ , and  $4 \times 4$  waveguide arrays, along with their different setup parameters, in which different wavelength values are simulated. Below Table 1 is representing the waveguide numbers, wavelengths considered, and other optimization parameters used in the simulation. The parameters and their values are shown in the following table:

**TABLE 1. Waveguide and Optimization System Setup.**

S. No.	Parameters	Values
1	Waveguide arrays	2x2, 3x3, 4x4
2	Simulated Wavelengths	3.1 - 3.6 $\mu\text{m}$ , 640-690 nm
3	Reflectivity	0.2
4	Iterations	20
5	Population Size	20
<b>Coefficients for Proposed HLGOS-PSGSA based model</b>		
1	Gravitational Constant	100
2	Accelerate Constants	c1=4, c2=2
3	Inertia Weight	0.12
<b>Coefficients for PSO based model</b>		
1	Inertia Weight	0.2
2	Inertia Factor	0.7
3	Accelerate Constants	c1= c2 =2
<b>Coefficients for FA based model</b>		
1	Light Absorption Coefficient	1
2	Attraction Coefficient	2
3	Mutation Coefficient	0.2
<b>Coefficients for GSA based model</b>		
1	Gravitational Constant	100
2	$\alpha$	20

These waveguides are analyzed and simulated by considering different parameters i.e. intensity, visibility, and 1/SNR.

### 1) INTENSITY

The intensity of the waveguide must be high. For  $m^{\text{th}}$  waveguide of length  $z = L$ , the peak intensity at the output is defined as:

$$I_m = \left\langle \left| \sum_{k=1}^N \alpha_{m,f(k)} A_k \right|^2 \right\rangle = \sum_{j=1}^N \sum_{k=1}^N \alpha_{m,f(j)} \alpha_{m,f(k)}^* \langle A_j A_k^* \rangle \quad (11)$$

where  $f(k)$  is the function, that maps  $k=1..N$  to the  $N \times N$  waveguide array sites, at which the fields  $A_k$  have been coupled.  $\alpha_{m,f(k)}$  coefficients are the mode amplitudes

at  $n^{\text{th}}$  waveguide end, when a unit power field has been injected into site  $f(k)$  at  $z = 0$  [45].

### 2) VISIBILITY

To attain a positive output, the visibility of the waveguide should also be high. For the fields which are completely synchronized, normalized visibility can be evaluated by:

$$V_{ij} = \sqrt{\frac{(\Re\langle A_i A_j^* \rangle)^2 + (\Im\langle A_i A_j^* \rangle)^2}{\langle A_i A_j^* \rangle \langle A_i A_j^* \rangle}} \quad i \neq j \quad (12)$$

where  $\Re$  and  $\Im$  are the real and imaginary parts of the product of the complex field [46].

### 3) 1/SNR

The third parameter considered for performance evaluation is 1/SNR, and it must be low for efficient output. It is defined as:

$$\frac{1}{SNR} = \sqrt{\frac{N-1}{2I_0}} \quad (13)$$

where  $N$  is the number of telescopes and  $I_0$  implies the intensity [47].

## V. RESULTS AND DISCUSSION

The performance of the proposed hybrid model is simulated and compared to several optimization techniques, along with the existing approach in the MATLAB Simulink software. The simulated outcomes are obtained for three different waveguides models i.e.  $2 \times 2$ ,  $3 \times 3$ , and  $4 \times 4$  in terms of different performance parameters which include magnification, normalized intensity, visibility, and 1/SNR. The detailed discussion of the achieved outcomes is discussed briefly in this section.

### A. FOR $2 \times 2$ WAVEGUIDE ARRAY

The proposed model for waveguide selection is firstly implemented using existing optimization algorithms such as PSO, FA, and GSA. After simulation, the results have been analyzed with the existing schemes. Finally, the proposed hybrid optimization algorithm is evaluated and compared with standard bar, cross, PSO, FA, and GSA models for  $2 \times 2$  waveguide array in terms of their normalized intensity at different wavelengths. Fig. 2 shows the comparison graph of the proposed model and other models at varying wavelengths.

Fig. 2 illustrates the graph obtained for normalized intensity in the  $2 \times 2$  waveguide model for traditional [48] and [50] approaches, proposed optimization-based models, and hybrid approach-based models. The value on the x-axis represents the value of different wavelengths starting from 3.1  $\mu\text{m}$  and goes up to 3.6  $\mu\text{m}$ . Whereas, the values on the y-axis represent the values for normalized intensity. From the graph, it is observed that the value of normalized intensity for total spectrum [50] is starting from 0.2 and with a high rise, get decreased with increase in wavelength, whereas, the traditional bar approach [48] is high in the beginning i.e. 0.75 and

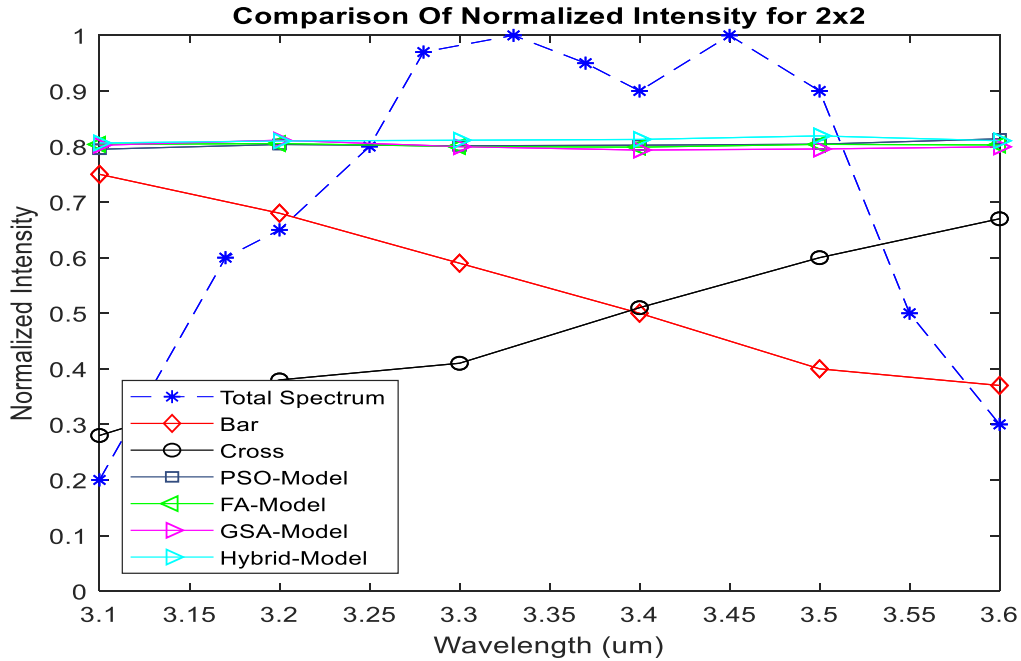


FIGURE 2. Comparison of normalized intensity for 2 × 2 waveguide array.

TABLE 2. comparison table of normalized intensity for 2 × 2.

Wavelength (um)	Total Spectrum ([46], [48])	Bar [43]	Cross [43]	PSO Model	FA Model	GSA Model	Hybrid Model
3.1	0.2	0.75	0.28	0.795086465	0.803867338	0.802249036	0.806423058
3.2	0.65	0.68	0.38	0.803709712	0.805345848	0.811442991	0.809995858
3.3	0.97	0.59	0.41	0.801278795	0.800127214	0.799779936	0.811316568
3.4	0.9	0.5	0.51	0.802429554	0.798890988	0.793622686	0.812754312
3.5	0.9	0.4	0.6	0.804189174	0.803922776	0.795558653	0.819139951
3.6	0.3	0.37	0.67	0.813934398	0.802830026	0.799484921	0.810369387

then starts decreasing gradually with the increased wavelength. The value of intensity at 3.6 μm is only 0.37. However, the value of intensity in the standard cross method [48] is only 0.28 in the beginning and then goes on increasing with the increase in wavelength and is 0.67 at 3.6 μm. The intensity of the cross approach is higher than the bar approach, but, it is not the best. The value of intensity achieved by the PSO, FA, and GSA approaches for the final wavelength of 3.6 μm came out to be 0.813934398, 0.802830026, and 0.7994849 respectively. However, in the case of our proposed hybrid model, the normalized value of intensity is higher than all the traditional methods i.e. 0.810369387 at 3.6 μm. The exact value of normalized intensity with the varying wavelength is mentioned in Table 2.

Similarly, the performance of the proposed hybrid model is also analyzed and compared in terms of visibility for 2 × 2 waveguides and is depicted in Fig. 3.

Fig. 3 represents the comparison graph of the proposed hybrid model and PSO, FA, and GSA models in terms of

their visibility power, for 2 × 2 waveguides with varying wavelengths. The value on the x-axis represents the value of different wavelengths, starting from 3.1 μm and goes up to 3.6 μm, whereas, the values on the y-axis show the values for visibility. From the graph, it is observed that visibility in the PSO model is varying with the change in wavelength values, and came out to be only 0.941255208 at 3.6 μm. However, the visibility values in FA and GSA models are 0.95203397 and 0.92302993 respectively, at 3.6 μm. On the other hand, the visibility in the suggested hybrid model is better than all the three traditional models and is equal to 0.981151775 at the last wavelength. From the graph, it is also analyzed that the varying wavelength doesn't affect the visibility power in the proposed model that much, and is improving with the increase in wavelength value. The specific values of visibility achieved by PSO, FA, and GSA models and the proposed HLGOS-PSGSA model for 2 × 2 waveguides with varying wavelengths are mentioned in Table 3.

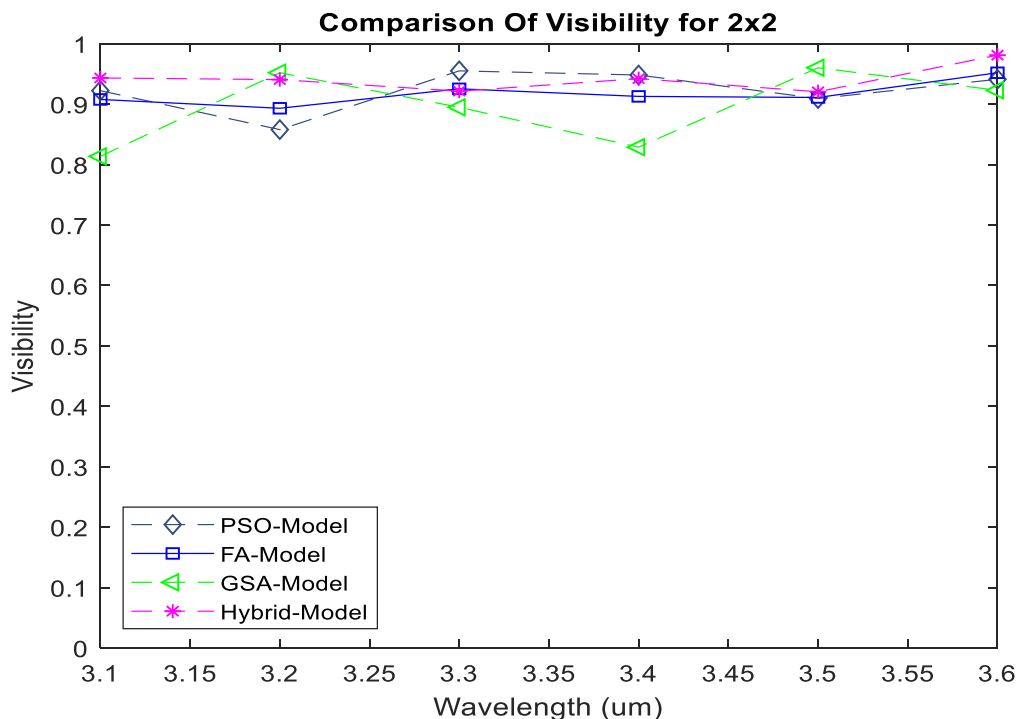


FIGURE 3. Comparison of visibility for 2 x 2 waveguide array.

TABLE 3. comparison table of Visibility for 2 x 2.

Wavelength (um)	PSO Model	FA Model	GSA Model	Hybrid Model
3.1	0.922362136	0.907869739	0.813702321	0.943425236
3.2	0.857932012	0.893245007	0.952208864	0.940707291
3.3	0.955167331	0.925476552	0.894907641	0.921599696
3.4	0.948305258	0.912915168	0.828930909	0.942261846
3.5	0.909352355	0.911150171	0.960328319	0.920577801
3.6	0.941255208	0.952033974	0.923029931	0.981151775

**B. FOR 3 x 3 WAVEGUIDE ARRAY**

The efficiency of the proposed hybrid model is then evaluated for a 3 x 3 waveguide setup and compared with the existing model [46]. Optimization algorithms (PSO, FA, and GSA) based models in terms of their intensity, visibility, minimum and maximum 1/SNR factors have been analyzed. Fig. 4 shows the comparison graph of the proposed and the other models in terms of normalized intensity for 3 x 3 waveguides.

Fig. 4, illustrates the comparison graph of the proposed hybrid model with the traditional model [46], and optimization-based waveguide selection models in terms of their normalized intensity values. The values on the x-axis and y-axis represent the wavelength and normalized intensity values respectively. From the obtained graph, it is analyzed that the normalized intensity value in the traditional model is very low, with starting range of 0.22.

The intensity keeps on varying with the change in wavelength, and finally, intensity equal to 0.19 has been achieved,

when the wavelength is equal to 690 nm. However, the intensity value in the later-on suggested optimization-based methods gets improved and came out to be 0.311765 initially in the PSO method, which then undergoes ups and downs, and at the end, reaches 0.05872 intensity value. Similarly, the normalized intensity value in FA and GSA is calculated with the changing wavelength value and came out to be 0.323196 and 0.316002 in the beginning when the wavelength is 640 nm, and increases with the increase in wavelength i.e. 0.33184 and 0.327109 respectively at 690 nm. While talking about the normalized intensity achieved in the proposed HLGOS-PSGSA model, that came out as 0.38139 at the beginning, which then keeps on increasing with slight variations, and finally, achieves a value of 0.385211 at 690 nm. Thus, the proposed hybrid model has the highest intensity for 3 x 3 waveguides. Table 4 shows the normalized intensity values of traditional, optimization-based approaches, and the proposed scheme for 3 x 3 waveguides.

In addition to this, an analysis of results for optimized and non-optimized schemes with the proposed model is also performed in terms of visibility for 3 x 3 waveguides through different wavelengths and is shown in Fig. 5.

Fig. 5 illustrates the comparison graph of the proposed hybrid model and standard PSO, FA, and GSA models in terms of their visibility power. From the obtained graph, it is analyzed that the visibility in traditional models starts from 0.4 with a wavelength of 640 nm and then goes up drastically and reaches the maximum value of 0.87, which later on decreases again to 0.39 with the further increase



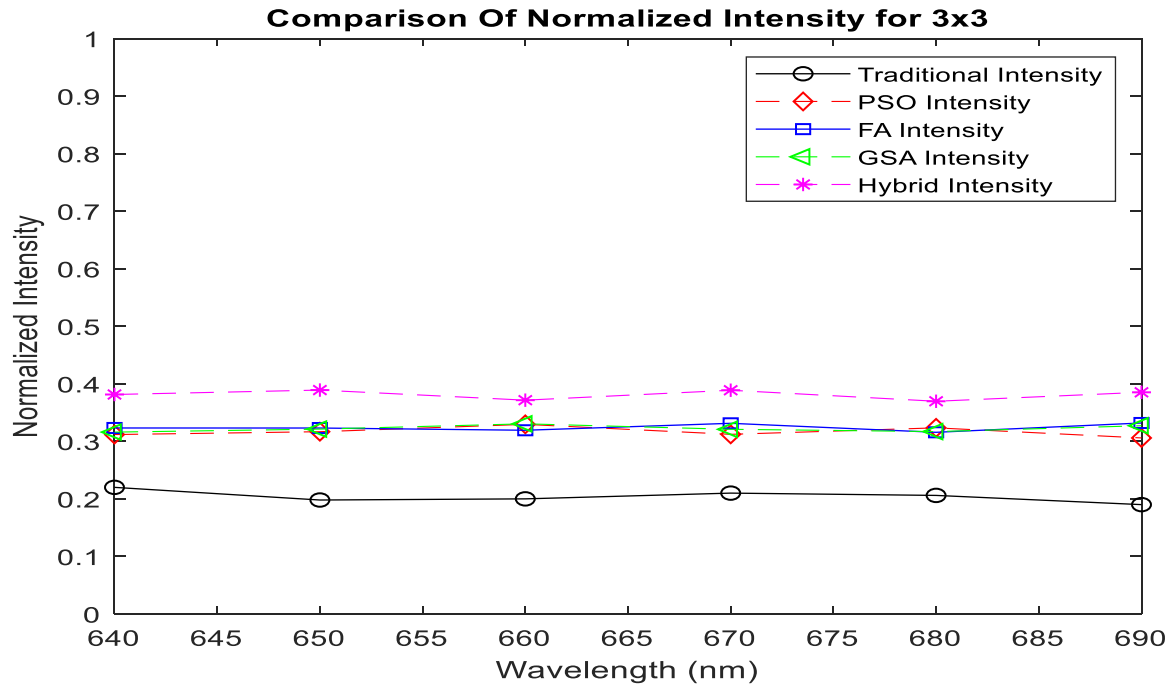


FIGURE 4. Comparison of normalized intensity for 3 x 3 waveguide array.

TABLE 4. comparison table of Normalized intensity for 3 x 3.

Wavelength (nm)	Traditional Model [44]	PSO Model	FA Model	GSA Model	Hybrid Model
640	0.22	0.311765	0.323196	0.316002	0.381390
650	0.198	0.316720	0.323115	0.321242	0.389077
660	0.2	0.329484	0.319228	0.330418	0.371520
670	0.21	0.312152	0.331319	0.320901	0.388792
680	0.206	0.323406	0.315676	0.316916	0.369622
690	0.19	0.305872	0.331840	0.327109	0.385211

in wavelength values. On the other hand, visibility in other standard models like PSO, FA, and GSA is much better than previous models. The visibility in the PSO model is 0.800389 in the beginning and then keeps on increasing with the increase in wavelength values and reaches 0.806387 when the wavelength value is 690 nm. However, in the case of the FA method, the visibility changes accordingly, i.e. it is higher in the beginning, i.e. 0.869144, and then starts to decrease with the rise in wavelength. When the wavelength value is maximum i.e. 690 nm, visibility in the FA model is only 0.788327. The same is the case in the GSA model, in which visibility is very high i.e. 0.897175 in the beginning when wavelength intensity is low, but, as soon as the value of wavelength increases, the visibility decreases, and finally ends up at 0.849266, when the wavelength is maximum at 690 nm. However, in the case of the proposed hybrid model, the value of visibility begins at 0.865186 and then goes on increasing with the increase in wavelength value. The visibility is 0.927665 in the proposed hybrid model with

690 nm of wavelength. The changing values of visibility in traditional models and proposed hybrid models at different wavelengths are mentioned in Table 5.

Moreover, the effectiveness of the proposed hybrid system is also evaluated and compared with the other models in terms of minimum and maximum values of 1/SNR at different wavelengths. Figures 6 and 7 show the comparison graph in terms of their minimum and maximum 1/SNR values.

In figures 6 and 7, the value on the x-axis and y-axis calibrate the varying wavelength and 1/SNR values respectively. From the graphs, it is analyzed that the min and max 1/SNR is highest for the PSO-based model when compared to other FA and GSA-based models. After analyzing Fig. 6 closely, it has been observed that in PSO models, the values of min 1/SNR are 0.133477, 0.141429, 0.13494, 0.134836, 0.139817, and 0.122482 at 640, 650, 660, 670, 680, and 690 nm, respectively. While in FA and GSA-based models, the values of min. 1/SNR are varying between 0.11 to 0.13, which is lesser than the PSO. Similarly, in Fig. 7, max 1/SNR values for

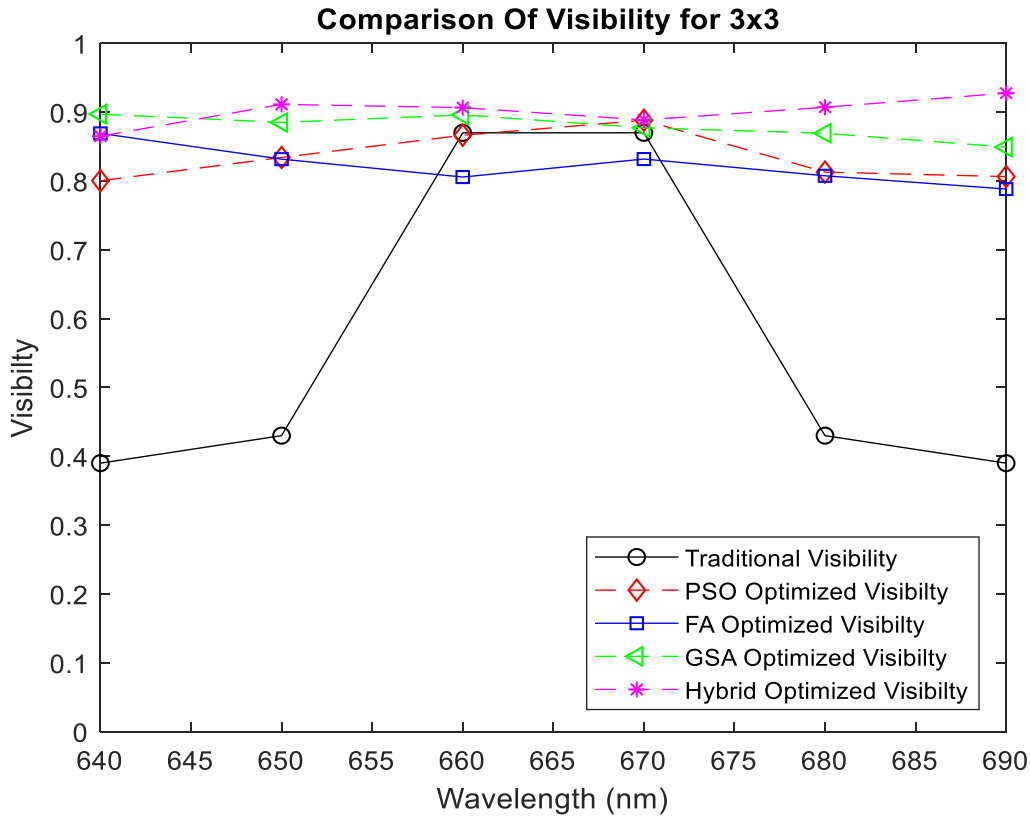


FIGURE 5. Comparison of visibility for 3 x 3 waveguide array.

TABLE 5. comparison of visibility for 3 x 3.

Wavelength (nm)	Traditional Model [44]	PSO Model	FA Model	GSA Model	Hybrid Model
640	0.39	0.800389	0.869144	0.897175	0.865186
650	0.43	0.834210	0.834210	0.885174	0.911388
660	0.87	0.866505	0.805748	0.896091	0.906622
670	0.87	0.888301	0.831924	0.877327	0.888646
680	0.43	0.812960	0.807565	0.869388	0.907203
690	0.39	0.806387	0.788327	0.849266	0.927665

PSO are mostly above 0.32, whereas, in the case of FA and GSA-based models, these are between 0.29 to 0.31. Among FA and GSA, GSA based model is performing better in terms of the 1/SNR factor. After analyzing these algorithms, when the proposed scheme is compared with them, 1/SNR values for the proposed scheme are comparatively lesser than all the 3 algorithms. The variation of the proposed scheme for both min and max 1/SNR factors is below 0.09 and 0.25. This strengthens the effective performance of the proposed scheme in achieving better visibility and intensity at low 1/SNR.

C. FOR 4 x 4 WAVEGUIDE ARRAY

Continuing the performance analysis of optimization algorithms for waveguide selection, finally, 4 x 4 waveguide

mode has been simulated and evaluated in terms of normalized intensity, visibility, and other performance factors. Fig. 8 shows the comparison graph of the traditional methods [49] and [51], PSO, FA, GSA-based optimized waveguide selection models, and the proposed hybrid model in terms of their normalized intensity. From the graph, it is observed that the values of intensities in the traditional model are very low, which makes them inconvenient and inefficient. However, after applying the optimization-based techniques such as PSO, FA, and GSA models, the value of intensity gets improved with their initial values 0.321274, 0.325997, and 0.379499 at 640 nm wavelength. The intensity then keeps on changing without following any proper pattern, but, with the least variation with values of 0.329836, 0.321452,

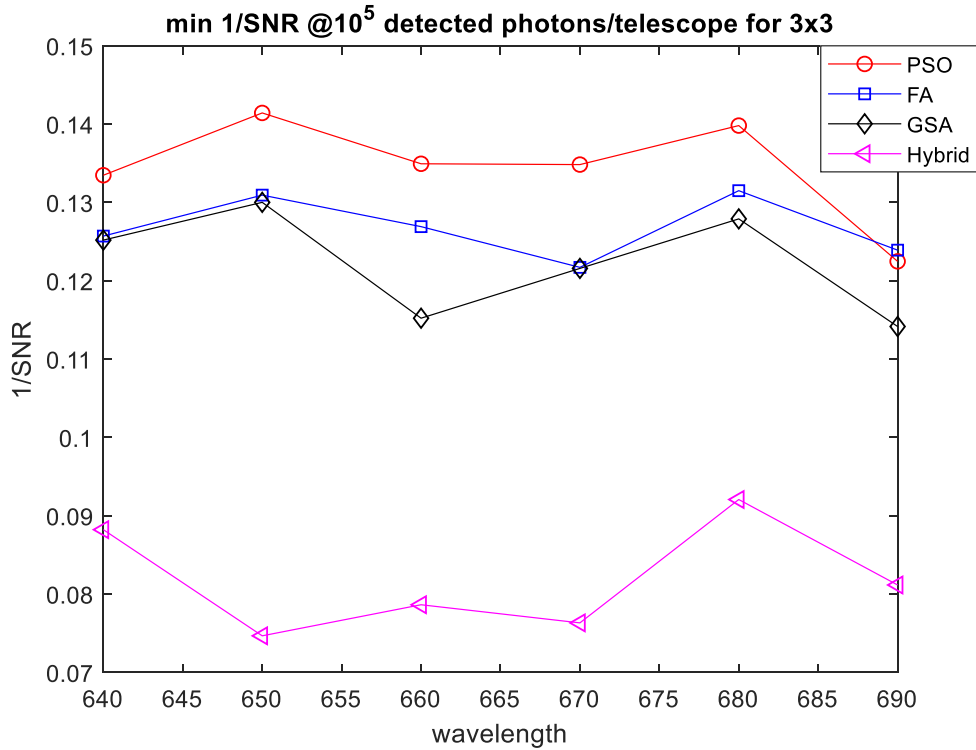


FIGURE 6. Comparison of min 1/SNR for 3 × 3 waveguide array.

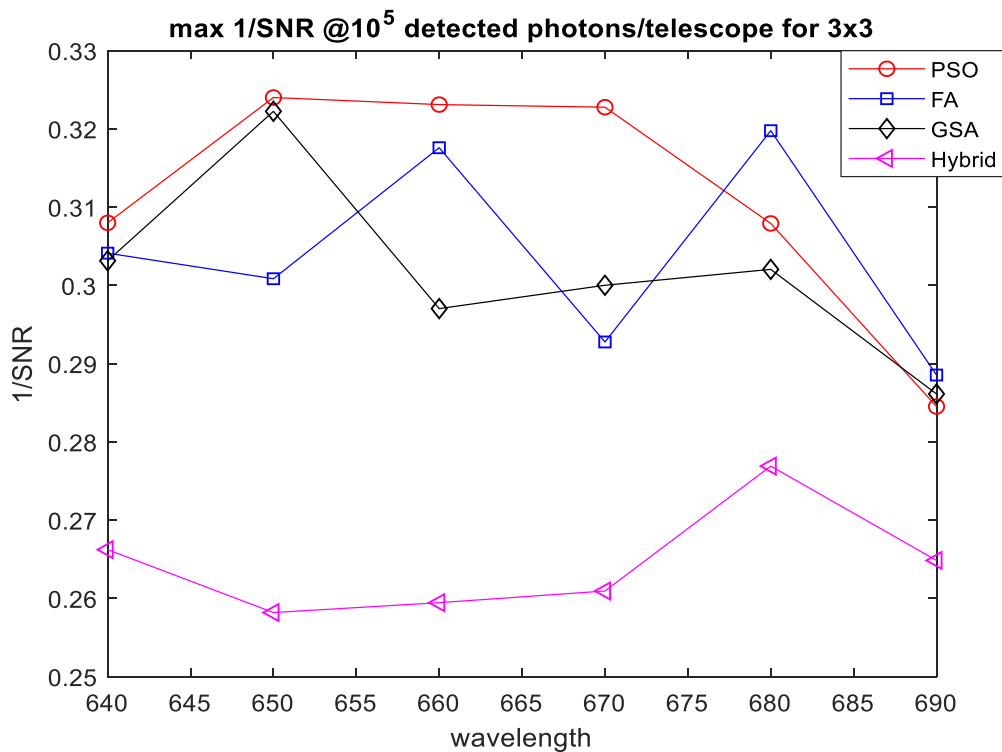


FIGURE 7. Comparison of max 1/SNR for 3 × 3 waveguide array.

and 0.315655 at 690 nm of wavelength, respectively. However, in the case of the proposed hybrid model,

the intensity gets much better i.e. 0.379499 than the other optimization-based models right from the beginning, where

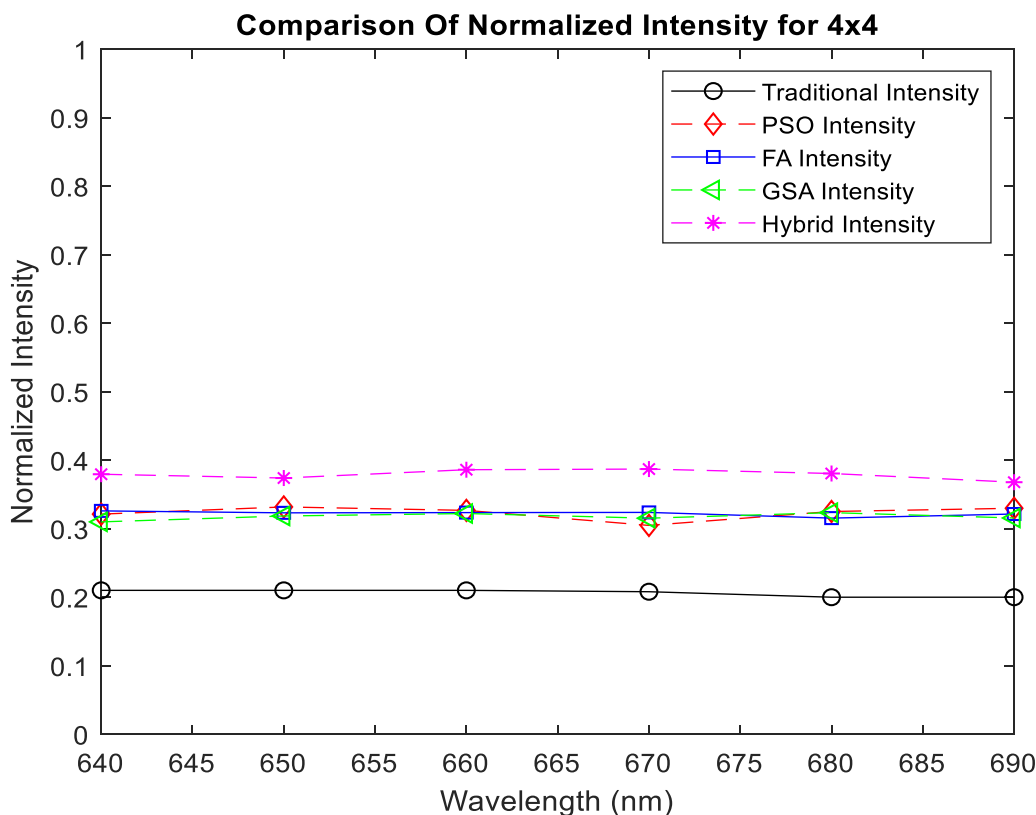


FIGURE 8. Comparison of normalized intensity for 4 × 4 waveguide array.

TABLE 6. comparison of Normalized Intensity for 4 × 4.

Wavelength (nm)	Traditional Model [47], [49]	PSO Model	FA Model	GSA Model	Hybrid Model
640	0.21	0.321274	0.325997	0.309951	0.379499
650	0.21	0.331751	0.323162	0.318546	0.373966
660	0.21	0.326739	0.323509	0.322152	0.386097
670	0.21	0.304797	0.323771	0.315350	0.387053
680	0.20	0.325110	0.315467	0.323434	0.380561
690	0.20	0.329836	0.321452	0.315655	0.367854

the wavelength is 640 nm, which keeps on fluctuating slightly with the increase in wavelength intensity and finally reaches 0.367854 at 690 nm of wavelength. The detailed value of normalized intensity achieved in the proposed and traditional model is mentioned in Table 6.

After analyzing the schemes in terms of intensity, visibility is evaluated for a 4 × 4 waveguide setup. Fig. 9 represents the comparison graph for 4 × 4 waveguides in terms of their visibility power. From the obtained graph, it has been analyzed that the visibility in PSO, FA, and GSA-based models vary according to the varying wavelength. When analyzed with a variation in wavelength between 640 to 690 nm, the visibility value achieved at 640 nm from the traditional models [49] and [51] is 0.75, whereas, PSO, FA, and GSA-based models are giving visibility values of 0.81, 0.86 and 0.87, respectively. The results show that the visibility achievement of

GSA based model is better than other models. In the proposed scheme, as both the features of PSO and GSA are there, the visibility values achieved are much improved and are reaching up to 0.9177 at 640 nm wavelength. On comparing the visibility at other wavelength values, the hybrid algorithm is achieving better results, followed by GSA, FA, and PSO-based models. Table 7 shows the values of visibility in the traditional and proposed models.

Finally, the performance of the proposed scheme is compared and analyzed in terms of 1/SNR. Figures 10 and 11 represent the comparison graphs of the proposed hybrid model and PSO, FA, and GSA-based models in terms of their min and max 1/SNR values for the 4 × 4 waveguide. From the obtained graphs, it has been analyzed that the lowest value of min 1/SNR is 0.14, 0.153, and 0.1514 at 650, 650, and 660 nm in the traditional PSO, FA, and GSA models.

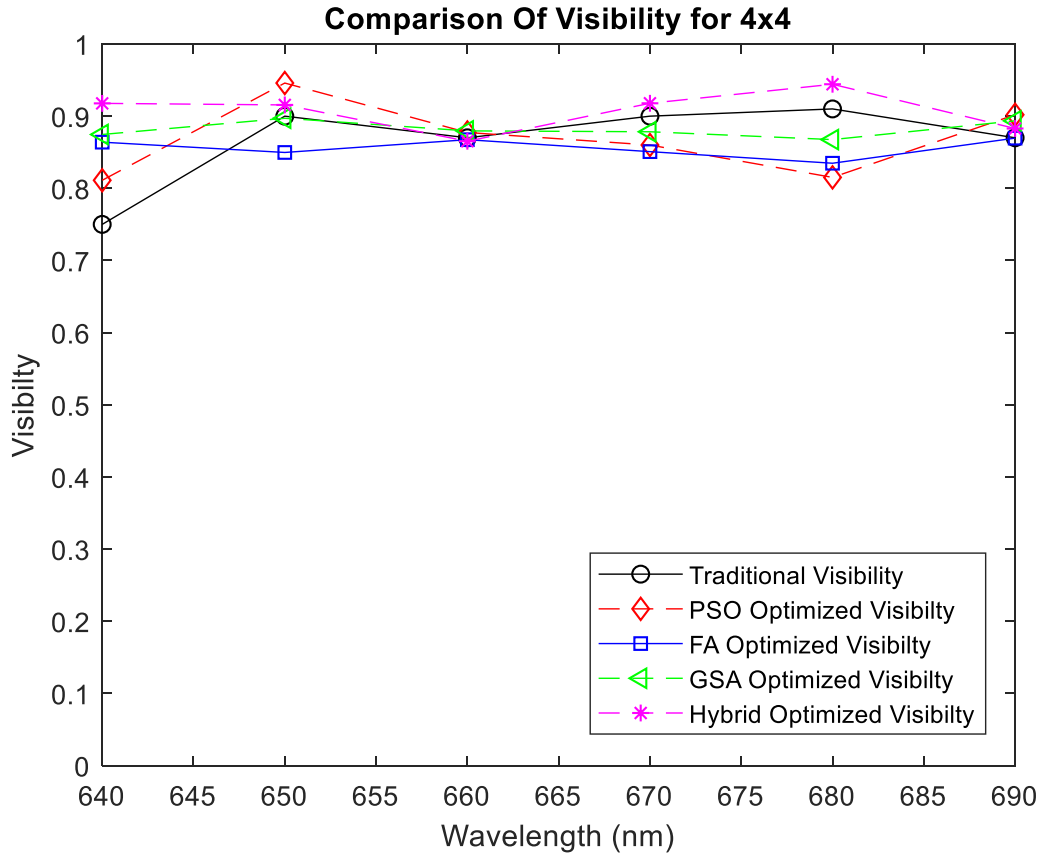


FIGURE 9. Comparison of visibility for 4 x 4 waveguide array.

TABLE 7. comparison of Visibility for 4 x 4.

Wavelength (nm)	Traditional Model [47], [49]	PSO Model	FA Model	GSA Model	Hybrid Model
640	0.75	0.811129	0.863954	0.874605	0.917718
650	0.90	0.945880	0.849674	0.897082	0.915556
660	0.87	0.877353	0.867373	0.879603	0.865267
670	0.90	0.859989	0.850791	0.878379	0.917841
680	0.91	0.815148	0.834761	0.867510	0.944202
690	0.87	0.901954	0.869535	0.893531	0.882896

However, in the proposed model, the lowest value for 1/SNR is obtained at 680 nm i.e. 0.100013. Similarly, the highest value of min. 1/SNR is achieved at 680, 640, and 640 nm with 0.163589, 0.165057, and 0.163248 respectively, in conventional PSO, FA, and GSA models. However, the highest value of min 1/SNR is achieved at 650 nm with a value of 0.112542. Similarly, the lowest and the highest value of max. 1/SNR is calculated, which comes out to be lowest at 680, 650, and 690 nm in conventional PSO, FA and GSA models with values 0.362073, 0.364045, and 0.364193, respectively. While in the proposed hybrid model, the lowest and the highest max1/SNR value is attained at 660 and 690 nm of wavelength with values 0.316945 and 0.364022, respectively.

VI. OVERALL COMPARISON FOR 3 SCENARIOS

After analyzing the results of traditional models and the proposed hybrid model, it has been observed that the proposed hybrid model is performing better for all three waveguides arrays in terms of intensity, visibility, and min and max 1/SNR. After combining the results of all the parameters, it is observed that for the 2 x 2 array, the normalized intensity and visibility are better in PSO based model among other optimization algorithms (FA and GSA), but the proposed model is giving better intensity and visibility with respect to PSO also. Similarly, for the 3 x 3 waveguide array, intensity is better in the FA method, but its visibility power is low. However, when we talk about PSO and GSA models, the intensity is slightly lower than the FA model, but, the value of visibility



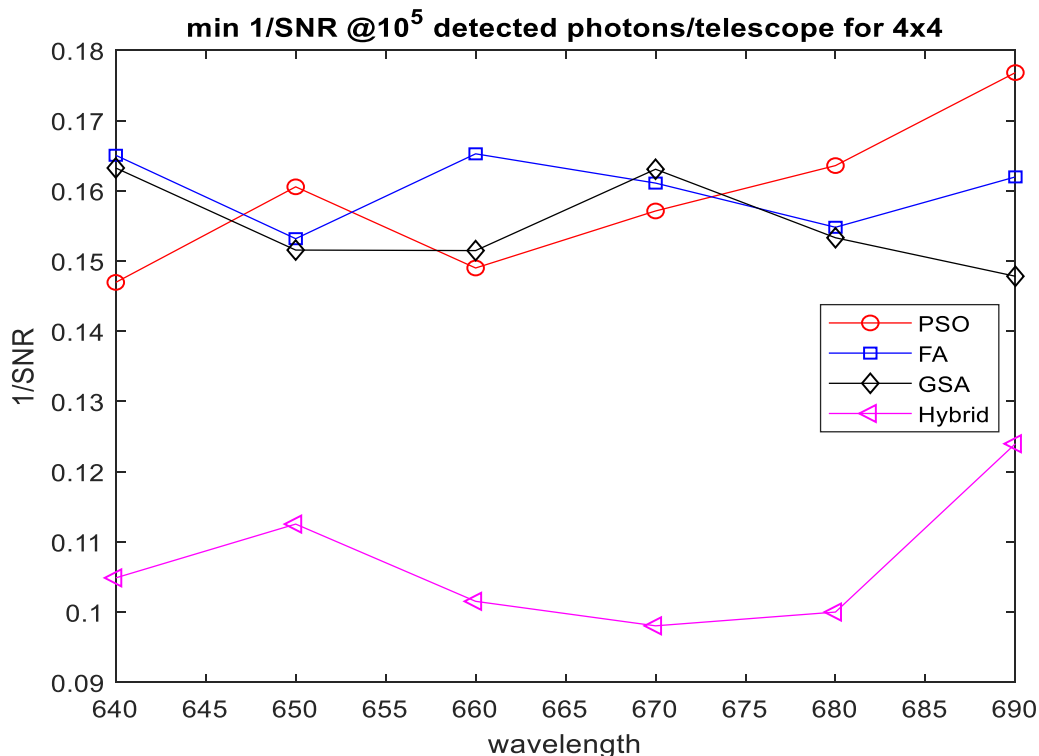


FIGURE 10. Comparison of min 1/SNR for 4 × 4 waveguide array.

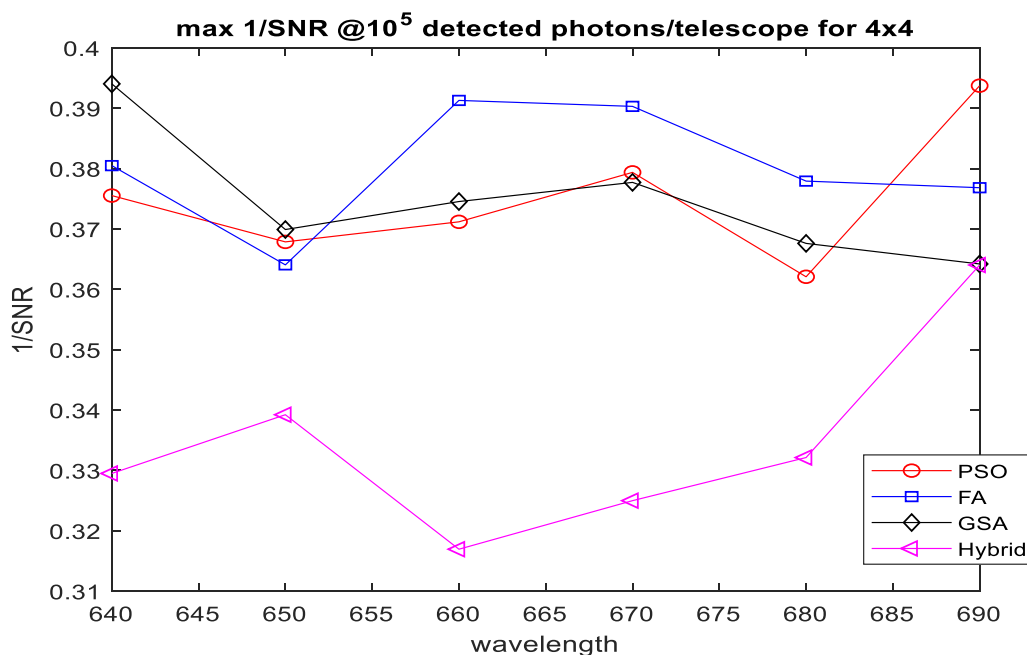


FIGURE 11. Comparison of max 1/SNR for 4 × 4 waveguide array.

is high in both models. However, when the intensity and visibility values of these models are compared with the proposed hybrid model, it is observed that the proposed model is performing more efficiently with varying wavelengths, both in terms of intensity and visibility. Likewise, for the

4 × 4 waveguide array, normalized intensity is good in PSO and FA-based models, and is low for GSA-based models, but the visibility is maximum in PSO and GSA models among 3 techniques based on PSO, FA, and GSA. However, when the intensity and visibility values are compared with the proposed

hybrid model, it is observed that the proposed hybrid model outperforms them in both parameters, thus, making it more efficient and convenient. In addition to this, the min and max 1/SNR value in the proposed hybrid model is very less than PSO, FA, and GSA-based models for both  $3 \times 3$  and  $4 \times 4$  waveguide simulations. Hence, it is concluded that the proposed hybrid model is more efficient, reliable, stable, and convenient among other optimization algorithms.

## VII. CONCLUSION

In this research work, a hybrid model of an interferometer based on PSO-GSA optimization, with waveguide selection from the waveguide array, is proposed to achieve high intensity and visibility output at the beam combiner. The implementation of the proposed hybrid PSO-GSA approach can be used for waveguide selection in the field of interferometry. The performance of the proposed hybrid model is evaluated in MATLAB simulation software. The simulation outcomes are obtained and compared with other state-of-the-art techniques for 3 different waveguide array combinations i.e.  $2 \times 2$ ,  $3 \times 3$ , and  $4 \times 4$ , in terms of different performance parameters, such as normalized intensity, visibility, and 1/SNR. From the results, it is analyzed that the visibility and normalized intensity values are best achieved in the proposed hybrid model for selecting waveguides, when compared with the traditional, and optimization-based models, including PSO, FA, and GSA. In addition to this, the efficiency of the proposed hybrid model is also analyzed in terms of the minimum and maximum 1/SNR values, which came out to be the lowest in the proposed hybrid model for all the three waveguide arrays i.e.  $2 \times 2$ ,  $3 \times 3$ , and  $4 \times 4$ , thus, making it more efficient model. Therefore, the proposed hybrid model outperforms the conventional and proposed optimization-based models in multiple performance factors, which makes it more effective and convenient to be adopted for beam combiners in interferometry.

## REFERENCES

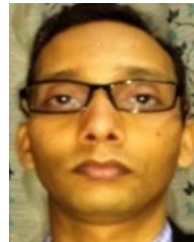
- [1] A. S. Nayak, T. Poletti, T. Sharma, K. Madhav, E. Pedretti, L. Labadie, and M. Roth, "Chromatic response of a four-telescope integrated-optics discrete beam combiner at the astronomical L band," *Opt. Exp.*, vol. 28, no. 23, pp. 34346–34361, Nov. 2020.
- [2] P. Hariharan, *Basics of Interferometry*, 2nd ed. Sydney, NSW, Australia: Academic, 2007.
- [3] A. Quirrenbach, "The development of astronomical interferometry," *Exp. Astron.*, vol. 26, pp. 49–63, Apr. 2009.
- [4] S. Minardi, "Nonlocality of coupling and the retrieval of field correlations with arrays of waveguides," *Phys. Rev. A, Gen. Phys.*, vol. 92, no. 1, pp. 1–7, Jul. 2015.
- [5] X. Luo, *Engineering Optics 2.0: A Revolution in Optical Theories, Materials, Devices and Systems*, 1st ed. Singapore: Springer, 2019, doi: [10.1007/978-981-13-5755-8](https://doi.org/10.1007/978-981-13-5755-8).
- [6] U. Röpke, H. Bartelt, S. Unger, K. Schuster, and J. Kobelke, "Fiber waveguide arrays as model system for discrete optics," *Appl. Phys. B, Lasers Opt.*, vol. 104, no. 3, pp. 481–486, Jul. 2011.
- [7] R. Marti, P. M. Pardalos, and M. G. Resende, "Genetic algorithms," in *Handbook of Heuristics*, 1st ed. Cham, Switzerland: Springer, Aug. 2018, pp. 431–464, doi: [10.1007/978-3-319-07153-4](https://doi.org/10.1007/978-3-319-07153-4).
- [8] S. Katoch, S. S. Chauhan, and V. Kumar, "A review on genetic algorithm: Past, present, and future," *Multimedia Tools Appl.*, vol. 80, pp. 8091–8126, Oct. 2020.
- [9] M. Wang, T. Ma, G. Li, X. Zhai, and S. Qiao, "Ant colony optimization with an improved pheromone model for solving MTSP with capacity and time window constraint," *IEEE Access*, vol. 8, pp. 106872–106879, Jun. 2020.
- [10] M. Dorigo and C. Blum, "Ant colony optimization theory: A survey," *Theor. Comput. Sci.*, vol. 344, nos. 2–3, pp. 243–278, 2005.
- [11] A. Sharma, A. Sharma, S. Choudhary, R. K. Pachauri, A. Shrivastava, and D. Kumar, "A review on artificial bee colony and its engineering applications," *J. Crit. Rev.*, vol. 7, no. 11, pp. 4097–4107, 2020. [Online]. Available: <http://www.jcreview.com/fulltext/197-1596854993.pdf?1631617815>
- [12] H. Kraiem, A. Flah, N. Mohamed, M. Alowaidi, M. Bajaj, S. Mishra, N. K. Sharma, and S. K. Sharma, "Increasing electric vehicle autonomy using a photovoltaic system controlled by particle swarm optimization," *IEEE Access*, vol. 9, pp. 72040–72054, 2021, doi: [10.1109/ACCESS.2021.3077531](https://doi.org/10.1109/ACCESS.2021.3077531).
- [13] G. Rivera, L. Cisneros, P. Sánchez-Solís, N. Rangel-Valdez, and J. Rodas-Osollo, "Genetic algorithm for scheduling optimization considering heterogeneous containers: A real-world case study," *Axioms*, vol. 9, no. 1, pp. 1–16, Mar. 2020.
- [14] M. N. A. Wahab, S. N. Meziani, and A. Atyabi, "A comprehensive review of swarm optimization algorithms," *PLoS ONE*, vol. 10, no. 5, pp. 1–36, May 2015.
- [15] G. Leguizamón and E. Alba, "Ant colony based algorithms for dynamic optimization problems," in *Metaheuristics for Dynamic Optimization (Studies in Computational Intelligence)*, vol. 433, E. Alba, A. Nakib, and P. Siarry, Eds. Berlin, Germany: Springer, 2013, pp. 189–210, doi: [10.1007/978-3-642-30665-5\\_9](https://doi.org/10.1007/978-3-642-30665-5_9).
- [16] S. Mohanty, S. Mohapatra, and S. Meko, "Ant colony optimization (ACO-Min) algorithm for test suite minimization," in *Progress in Computing, Analytics and Networking*, Mar. 2020, pp. 55–63.
- [17] K. Hussain, M. N. Mohd Salleh, S. Cheng, Y. Shi, and R. Naseem, "Artificial bee colony algorithm: A component-wise analysis using diversity measurement," *J. King Saud Univ.-Comput. Inf. Sci.*, vol. 32, no. 7, pp. 794–808, Sep. 2020.
- [18] K. Hussain, M. N. M. Salleh, S. Cheng, and Y. Shi, "Comparative analysis of swarm-based Metaheuristic algorithms on benchmark functions," in *Advances in Swarm Intelligence (Lecture Notes in Computer Science)*, vol. 10385, Y. Tan, H. Takagi, and Y. Shi, Eds. Cham, Switzerland: Springer, 2017, doi: [10.1007/978-3-319-61824-1\\_1](https://doi.org/10.1007/978-3-319-61824-1_1).
- [19] W.-F. Gao, L.-L. Huang, S.-Y. Liu, F. T. S. Chan, C. Dai, and X. Shan, "Artificial bee colony algorithm with multiple search strategies," *Appl. Math. Comput.*, vol. 271, pp. 269–287, Nov. 2015.
- [20] P. Shao, L. Yang, L. Tan, G. Li, and H. Peng, "Enhancing artificial bee colony algorithm using refraction principle," *Soft Comput.*, vol. 24, no. 20, pp. 15291–15306, Mar. 2020.
- [21] A. Kaveh, S. Talatahari, and N. Khodadadi, "Stochastic paint optimizer: Theory and application in civil engineering," *Eng. With Comput.*, vol. 36, pp. 1–32, Oct. 2020, doi: [10.1007/s00366-020-01179-5](https://doi.org/10.1007/s00366-020-01179-5).
- [22] H. Karami, M. V. Anaraki, S. Farzin, and S. Mirjalili, "Flow direction algorithm (FDA): A novel optimization approach for solving optimization problems," *Comput. Ind. Eng.*, vol. 156, Jun. 2021, Art. no. 107224.
- [23] N. Rathee and R. S. Chhillar, "Gravitational search algorithm: A novel approach for structural test path optimization," *J. Interdiscipl. Math.*, vol. 23, no. 2, pp. 471–480, May 2020, doi: [10.1080/09720502.2020.1731960](https://doi.org/10.1080/09720502.2020.1731960).
- [24] P. Mohanty, R. K. Sahu, and S. Panda, "A novel hybrid many optimizing liaisons gravitational search algorithm approach for AGC of power systems," *Automatika, J. Control, Meas., Electron., Comput. Commun.*, vol. 61, no. 1, pp. 158–178, Jan. 2020.
- [25] G. Sun and A. Zhang, "A hybrid genetic algorithm and gravitational search algorithm for image segmentation using multilevel thresholding," in *Pattern Recognition and Image Analysis (Lecture Notes in Computer Science)*, vol. 7887, J. M. Sanches, L. Micó, and J. S. Cardoso, Eds. Berlin, Germany: Springer, 2013, pp. 707–714.
- [26] Y. Wang, S. Gao, Y. Yu, Z. Wang, J. Cheng, and T. Yuki, "A gravitational search algorithm with chaotic neural oscillators," *IEEE Access*, vol. 8, pp. 25938–25948, Feb. 2020.
- [27] H. Deghbouch and F. Debbat, "Hybrid bees algorithm with grasshopper optimization algorithm for optimal deployment of wireless sensor networks," *Inteligencia Artif.*, vol. 24, no. 67, pp. 18–35, Feb. 2021.
- [28] Y. Che and D. He, "A hybrid whale optimization with seagull algorithm for global optimization problems," *Math. Problems Eng.*, vol. 2021, pp. 1–31, Jan. 2021.

- [29] M. H. Mansor, R. M. S. R. Kecek, I. Musirin, N. A. Rahmat, M. S. A. Rahman, N. Roslan, M. N. Abdullah, S. A. Shaaya, and N. F. A. B. Aziz, "A hybrid optimization technique for solving economic dispatch problem," *J. Phys., Conf. Ser.*, vol. 1049, no. 1, pp. 1–7, Jul. 2018.
- [30] J. Ding, Q. Wang, Q. Zhang, Q. Ye, and Y. Ma, "A hybrid particle swarm optimization-cuckoo search algorithm and its engineering applications," *Math. Problems Eng.*, vol. 2019, pp. 1–12, Mar. 2019.
- [31] T. Nguyen-Trang, T. Nguyen-Thoi, T. Truong-Khac, A. T. Pham-Chau, and H. Ao, "An efficient hybrid optimization approach using adaptive elitist differential evolution and spherical quadratic steepest descent and its application for clustering," *Sci. Program.*, vol. 2019, pp. 1–15, Feb. 2019.
- [32] S. Mirjalili and S. Z. M. Hashim, "A new hybrid PSOGSA algorithm for function optimization," in *Proc. Int. Conf. Comput. Inf. Appl. (ICCIA)*, Dec. 2010, pp. 373–377.
- [33] N. Singh, S. Singh, and S. B. Singh, "A new hybrid MGBPSO-GSA variant for improving function optimization solution in search space," *Evol. Bioinf.*, vol. 13, pp. 1–13, Mar. 2017.
- [34] M. Saleh, F. Imansyah, U. A. Gani, and Hardiansyah, "Hybrid PSO-GSA technique for environmental/economic dispatch problem," *Int. J. Emerg. Res. Manage. Technol.*, vol. 6, no. 9, pp. 112–118, Sep. 2017.
- [35] M. Panda, P. P. Sarangi, and A. Sahu, "A hybrid PSOGSA algorithm for search based test data generation," Project Softw. Test., IIT Kanpur, Kanpur, India, Tech. Rep., Oct. 2015.
- [36] I. Koochi and V. Z. Groza, "Optimizing particle swarm optimization algorithm," in *Proc. IEEE 27th Can. Conf. Electr. Comput. Eng. (CCECE)*, May 2014, pp. 1–5.
- [37] N. K. Jain, U. Nangia, and J. Jain, "A review of particle swarm optimization," *J. Inst. Eng. India B*, vol. 99, pp. 407–411, Mar. 2018.
- [38] E. Rashedi, E. Rashedi, and H. Nezamabadi-Pour, "A comprehensive survey on gravitational search algorithm," *Swarm Evol. Comput.*, vol. 41, pp. 141–158, Jun. 2018.
- [39] R. García-Ródenas, L. J. Linares, and J. A. López-Gómez, "A memetic chaotic gravitational search algorithm for unconstrained global optimization problems," *Appl. Soft Comput.*, vol. 79, pp. 14–29, Jun. 2019.
- [40] T. A. Khan, S. H. Ling, and A. S. Mohan, "Advanced gravitational search algorithm with modified exploitation strategy," in *Proc. IEEE Int. Conf. Syst., Man Cybern. (SMC)*, Oct. 2019, pp. 1056–1061.
- [41] J. Wang, M. Zhang, H. Song, Z. Cheng, T. Chang, Y. Bi, and K. Sun, "Improvement and application of hybrid firefly algorithm," *IEEE Access*, vol. 7, pp. 165458–165477, Nov. 2019.
- [42] M. Bajaj and A. Kumar Singh, "Hosting capacity enhancement of renewable-based distributed generation in harmonically polluted distribution systems using passive harmonic filtering," *Sustain. Energy Technol. Assessments*, vol. 44, Apr. 2021, Art. no. 101030, doi: 10.1016/j.seta.2021.101030.
- [43] W. Pei, G. Huayu, Z. Zheqi, and L. Meibo, "A novel hybrid firefly algorithm for global optimization," in *Proc. IEEE 4th Int. Conf. Comput. Commun. Syst. (ICCCS)*, Feb. 2019, pp. 164–168.
- [44] S. Maza and D. Zouache, "Binary firefly algorithm for feature selection in classification," in *Proc. Int. Conf. Theor. Applicative Aspects Comput. Sci. (ICTAACS)*, Dec. 2019, pp. 1–6.
- [45] S. Minardi, "Photonic lattices for astronomical interferometry," *Monthly Notices Roy. Astronomical Soc.*, vol. 422, no. 3, pp. 2656–2660, May 2012.
- [46] S. Minardi, F. Dreisow, S. Nolte, and T. Pertsch, "Discrete beam combiners: Exploring the potential of 3D photonics for interferometry," *Proc. SPIE*, vol. 8445, Jul. 2012, Art. no. 844516.
- [47] R. Errmann and S. Minardi, "6- and 8-telescope discrete beam combiners," *Proc. SPIE*, vol. 9907, Aug. 2016, Art. no. 990733.
- [48] L. Labadie, S. Minardi, J. Tepper, R. Diener, B. Muthusubramanian, J. U. Pott, S. Nolte, S. Gross, A. Arriola, and M. Withford, "Photonics-based mid-infrared interferometry: 4-year results of the ALSI project and future prospects," *Proc. SPIE*, vol. 10701, Jul. 2018, Art. no. 107011R.
- [49] S. Minardi, A. Saviuk, F. Dreisow, S. Nolte, and T. Pertsch, "Discrete beam combiners: 3D photonics for future interferometers," *Haute Provence Observatory Colloq.*, vol. 23, no. 27, pp. 121–130, Sep. 2013.
- [50] J. Tepper, R. Diener, L. Labadie, S. Minardi, S. Gross, A. Arriola, M. Withford, and S. Nolte, "Photonics-based mid-infrared interferometry: The challenges of polychromatic operation and comparative performances," *Proc. SPIE*, vol. 10701, Apr. 2019, Art. no. 107011B.
- [51] S. Minardi, A. Saviuk, F. Dreisow, S. Nolte, and T. Pertsch, "3D-integrated beam combiner for optical spectro-interferometry," *Proc. SPIE*, vol. 9146, Jul. 2014, Art. no. 91461D.
- [52] B. Song, Z. Wang, L. Zou, L. Xu, and F. E. Alsaadi, "A new approach to smooth global path planning of mobile robots with kinematic constraints," *Int. J. Mach. Learn. Cybern.*, vol. 10, no. 1, pp. 107–119, Jan. 2019.
- [53] X. Li, D. Wu, J. He, M. Bashir, and M. Liping, "An improved method of particle swarm optimization for path planning of mobile robot," *J. Control Sci. Eng.*, vol. 2020, pp. 1–12, May 2020.
- [54] J. Jiang, X. Yang, X. Meng, and K. Li, "Enhance chaotic gravitational search algorithm (CGSA) by balance adjustment mechanism and sine randomness function for continuous optimization problems," *Phys. A, Stat. Mech. Appl.*, vol. 537, Jan. 2020, Art. no. 122621.
- [55] J.-S. Wang and S.-X. Li, "An improved grey wolf optimizer based on differential evolution and elimination mechanism," *Sci. Rep.*, vol. 9, no. 1, pp. 1–21, May 2019.



**SIMARPREET KAUR** received the B.Tech. and M.Tech. degrees from Punjab Technical University, Jalandhar, India, in 2001 and 2008, respectively. She is currently pursuing the Ph.D. degree in electronics and communication engineering with I. K. Gujral Punjab Technical University, Jalandhar. She is currently working as the Head of the Department of Electronics and Communication Engineering, Baba Banda Singh Bahadur Engineering College, Fatehgarh Sahib, Punjab.

She has also worked as a Lecturer with Punjab Engineering College, Chandigarh, India, for six years. She has more than 18 years of teaching experience. She has more than 60 research publications in leading national and international journals and conferences. Her current research interests include beam combiners, performance analysis of interferometers, optimization techniques, wireless sensor networks, and labview.



**MOHIT SRIVASTAVA** received the B.Tech. degree in electronics and communication engineering from Magadh University, Bodh Gaya, in 2000, the M.Tech. degree in digital electronics and systems from K.N.I.T. Sultanpur, in 2008, and the Ph.D. degree in image processing and remote sensing from the Indian Institute of Technology Roorkee, in 2013. He is currently a Professor with the Department of Electronics and Communication Engineering and the Research and Development Dean of Chandigarh Engineering College, Landran, Mohali, Punjab, India. He has more than 19 years of work experience in various environments, including industry, as well as educational and research centers. He has completed two IEDC (DST) funded projects. He has published more than 35 technical research papers in national and international journals, conferences, and seminars. His current research interests include digital image and speech processing, remote sensing and their applications in land cover mapping, and communication systems.



**NAVEEN KUMAR SHARMA** (Senior Member, IEEE) received the B.Tech. degree in electrical and electronics engineering from Uttar Pradesh Technical University Lucknow, Uttar Pradesh, in 2008, and the M.Tech. and Ph.D. degrees in power system from the National Institute of Technology Hamirpur, Himachal Pradesh, India, in 2010 and 2014, respectively. He worked as a Lecturer with the Department of Electrical Engineering, National Institute of Technology Hamirpur, from March 2014 to May 2017. He is currently an Assistant Professor with the Department of Electrical Engineering, I. K. Gujral Punjab Technical University, Main Campus, Kapurthala, Punjab. He has published several research papers in leading international journals and conference proceedings and presented papers at several prestigious academic conferences, such as IEEE and Springer. His research interests include the area of power market, renewable energy sources, power system optimization, and condition monitoring of transformers.



**KAMALJIT SINGH BHATIA** (Senior Member, IEEE) has been working as an Associate Professor with the ECE Department, G. B. Pant Institute of Engineering & Technology, Pauri Garhwal (an Autonomous Institute of Government of Uttarakhand), since May 2019. He has more than 18 years of experience in many prestigious colleges and universities in India. He has over 120 research publications in leading international and national journals and conferences. He has authored four professional/engineering text books. His current research interests include coded direct detected optical-OFDM systems, to design an optical OFDM system using different dimensional codes, to analyze the value of RIN (relative intensity to noise) for optical-OFDM systems, to improve the PAPR by mitigating fiber non-linearities, and to analyze the performance of back to back, amplitude-phase modulated optical OFDM systems. He is a Life Member of the Optical Society of America (OSA), ISTE, and Punjab Academy of Sciences. He has been the Technical Expert of Punjab Technical University, since 2010.



**FRIE AYALEW YIMAM** received the B.Sc. degree in electrical and computer engineering (power engineering) from Ambo University, in 2016, and the M.Sc. degree in power system engineering from Addis Ababa Science and Technology University. She has 12 publications and other three articles are under process. She is currently serving different international journals as an advisory board member/editor and a reviewer.



**HARSIMRAT KAUR** received the B.Tech. degree from IKGPTU, Jalandhar, Punjab, India, and the M.Tech. and Ph.D. degrees from the ECE Department, Sant Longowal Institute of Engineering and Technology, Longowal, Punjab. She is currently working as an Associate Professor with CTIEMT, Shahpur, Jalandhar. She has published many research papers in national/international journals and conferences. Her research interests include the synthesis of nano-materials, the composition of ferrite substrates, and their analysis using characterization techniques XRD, SEM, FTIR, and VNA.



**MOHIT BAJAJ** (Member, IEEE) was born in Roorkee, India, in 1988. He received the bachelor's degree in electrical engineering from the FET, Gurukula Kangri Vishwa Vidhyalya, Haridwar, India, in 2010, and the M.Tech. degree in power electronics and ASIC design from NIT Allahabad, Uttar Pradesh, India, in 2013. He is currently pursuing the Ph.D. degree with the Department of Electrical and Electronics Engineering, NIT Delhi, India. He has academic experience of five years. He has published over 30 research articles in reputed journals, international conferences, and book chapters. His research interests include power quality improvement in renewable DG systems, distributed generations planning, application of multi-criteria decision-making in power systems, custom power devices, the IoT, and smart grids.

...